A New Strategy for Scanning Hot Electron Microscopy

[1]N. Machida, K. Furuya, T. Hirata, and K. Mae

Department of Physical Electronics, Graduate School of Science and Engineering, Tokyo Institute of Technology, 2-12-1 O-okayama, Meguro-ku, Tokyo 152-8552, Japan

ABSTRUCT: A new strategy to observe hot-electron interference/diffraction in solid employing a scanning probe is presented. We use a ballistic electron emission microscopy (BEEM) configuration with a buried ultra-fine artificial structure causing hot-electron interference under a surface. The reciprocity theorem for quantum electron wave serves us a detection principle for sub-surface hot-electron interference by using BEEM experiment configuration. Numerical simulations of the new detection experiments are performed and a possible experimental set-up is clarified.

1. Introduction

By using transverse degrees of freedom of electron quantum waves, there could be realized a new functional device, *electron wave device* [1]. In the electron wave device, hot-electron plane waves are ejected from hot-electron emitter and those wavefronts are modulated by ultra-fine artificial semiconductor structures and thereby interference, diffraction, or wavefront transform occurs. To realize the electron wave device, it is the first priority to observe hot-electron interference/diffraction in solid-state structure. However, in general, pitch of interference pattern is so small that we must carefully devise a particular detection system for hot-electron interference.

A scanning hot-electron microscope (SHEM) is proposed as a tool to detect interference patterns of hot electron caused by ultra-fine artificial structure under a solid surface [2]. In SHEM, hot-electron interference caused by artificial wavefront modulator under a solid surface is detected by a scanning probe and highly resolved detection of hot-electron interference could be done. Since current component into the probe is not only hot electron signal but includes tunneling current, which is necessary to perform feed-back operations, we must distinguish the two current components by using such as a lock-in amplification. However, the amplitude of tunneling current is so large, about three orders larger than that of hot-electron signal, that current noise associated with the tunneling current easily mask the hot-electron signal derived by the sophisticated detection method and observation of hot-electron interference by the conventional SHEM has not yet been achieved.

Therefore, in this paper, we propose a new strategy for SHEM. The new strategy is based on the ballistic electron emission microscopy (BEEM) and the reciprocity of quantum mechanics.

[1] nmachida@pe.titech.ac.jp

Numerical experiments for the new SHEM are performed with realistic device conditions and possible experimental set-up is clarified.

2. The Experiment Method

In this section, we briefly introduce our new strategy for SHEM. Figure 1 shows a conceptual figure to explain our observation principle. As an interference device, we adopt a phase shifter, which cause phase difference of π between phases of electrons which passed through the shifter and not, and, thus, there appears an interference patterns with a dip as shown in the left side of Fig. 1 for a plane wave incidence. Discussions of interference by phase shifter are given in detail in the next section.

The quantum reciprocity enables us to do the following scenario. We eject electron flux from a point source on one side of device boundary, and measure current flowing into the other side of the device boundary. When we sweep the position of point source and measure the current at each source position, the current variation against source position exhibits just an interference pattern that appears when plane wave is incident into the electron wave device but the incident and detection plane replace each other (Fig. 1). Note that, in the point source experiment, we need an energy high-pass filter, which is a thick energy barrier with a barrier height to coincide with incident electron energy. Proof of our observation principle is briefly described in appendix. As a movable point source we adopt a scanning probe and, thus, our new strategy is a BEEM experiment for hot-electron interference.

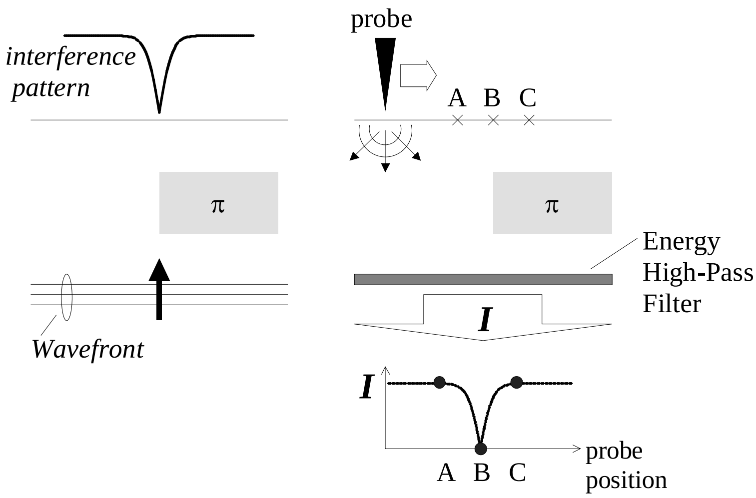

Figure 1: A conceptual figure to explain basic principle of our new SHEM

3. Numerical Experiment of New SHEM and Discussions

In this section, we perform numerical experiment of new SHEM taking realistic device situations into consideration. In Fig. 2, we show cross-sections of band profile at equilibrium for our device. Both phase shifter and energy filter is made of InP and another region is GaInAs except for Au base. An energy filter of 33 nm, a phase shifter of 11 nm, and a spacing between the filter and shifter of 6.5 nm (antireflection coating) are assumed by the premise that electron wavelength is 11 nm. A p-type delta-doping layer is inserted at z=100 nm. A flat band and inclined band variations can be attained by changing delta-doping density. Since we adopt InP material for both phase shifter and energy filter, it is better to incline a band, in order to acquire the filter characteristic near an ideal.

Figure 3 shows a result of new SHEM experiment when electron wavelength is 11 nm and the band is inclined so that a potential height at the edge of the energy filter is the same as electron energy (840 meV in Fig. 2). The horizontal axis is the probe position and vertical axis is the BEEM current. The numerical data is derived by the FDTD method [3]. The phase shifter lies in the negative region. From the figure, we can recognize an effective filtering performance and enough visible contrast for experimental observation.

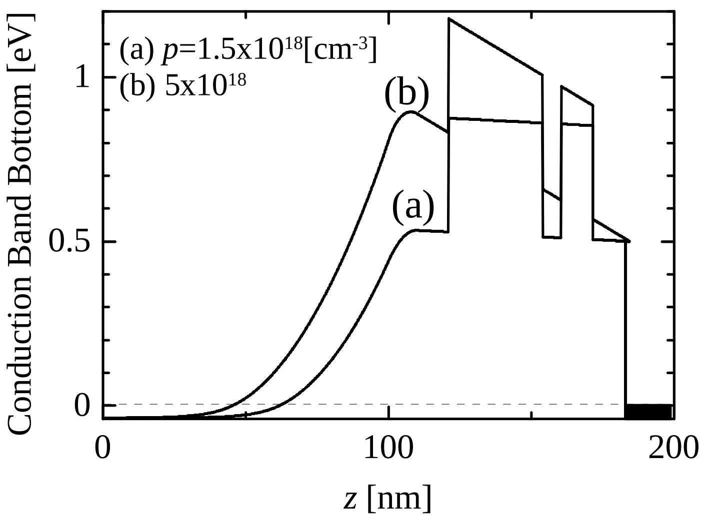

Figure 2: Calculated band profile inside the device

4. Conclusion

We have proposed a new strategy for SHEM. Numerical experiments for the new SHEM are performed with realistic device conditions and possible experimental set-up is clarified.

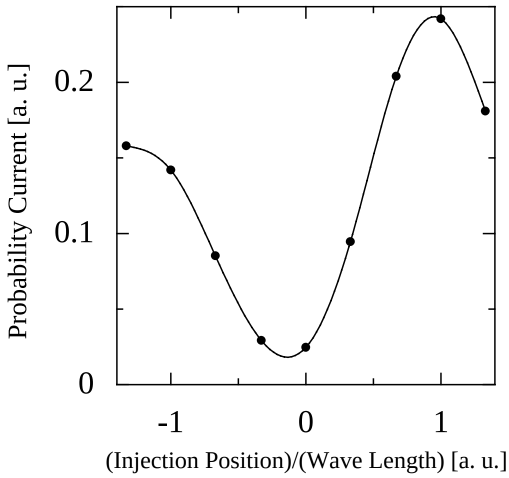

Figure 3: A numerical result of new SHEM experiment

References

[1] K. Furuya: J. Appl. Phys., **62** (1987) 492.

[2] F. Vazquez, D. Kobayashi, I. Kobayashi, Y. Miyamoto, K. Furuya, T. Maruyama, M. Watanabe, and M. Asada: Appl. Phys. Lett., **69** (1996) 2196.

[3] H-S. Tsai: "***REAL TIME***", (CRC PRESS 2000).

[4] S. Datta: "*Electronic Transport in Mesoscopic Systems*", (Cambridge University Press, Cambridge, 1995).

Appendix: Proof of Observation Principle of New SHEM

In this appendix, we make a brief proof of observation principle of the new SHEM. The principle is due to the reciprocity of quantum mechanics and we will neglect any dephasing. We model electron transport in electron wave devices as in Fig. A-1. Generally, electron transport in electron wave devices can be described in terms of *S*-matrices [4]. For each electron total energy *E,* incoming wave amplitude *a* and outgoing wave amplitude *b* are related through a scattering matrix as

$$\{b\} = [S]\{a\}, \qquad \text{(A.1)}$$

where $\{a\}$ and $\{b\}$ are column vectors consisting of incoming and outgoing wave amplitudes of all the transverse modes in the terminals. $[S]$ is the *S*-matrix and because of reciprocity of quantum mechanics, *S*-matrix elements satisfy the relations

$$s_{mn} = s_{nm}, \qquad \text{(A.2)}$$

where s_{ij} is a (i,j) element of the *S*-matrix [4]. If we launch a wave with mode index n into electron wave device, usually we would like to see interference pattern with fundamental mode incidence, that is, n=0, then interference patter at detection plane is

$$\left|\psi_{2\leftarrow 1}(x)\right|^2 = \sum_{\alpha,\beta} s_{\alpha 0}{}^{*} s_{\beta 0}\chi_\alpha(x)\chi_\beta(x), \tag{A.3}$$

where χ_α is a transverse mode in the terminal 2 with mode index α. Next, we consider a situation where electron wave is ejected from spatially localized point x_0 on the detection plane in the terminal 2. Because of completeness of function set χ_αs, the delta function can be expressed as

$$\delta(x - x_0) = \sum_{\alpha} \chi_\alpha(x_0)\chi_\alpha(x). \tag{A.4}$$

Then, electron wave function at terminal 1 from point source at x_0 in the terminal 2 can be expressed by S-matrix as

$$\psi_{1\leftarrow 2}(x; x_0) = \sum_{\alpha} s_{n\alpha}\chi_\alpha(x_0)\phi_n(x), \tag{A.5}$$

whrere $\phi_n(x)$ is a nth transverse mode in terminal 1. Then, a total current flowing into terminal 1 is proportional to

$$\int\left|\psi_{1\leftarrow 2}(x; x_0)\right|^2 dx = \sum_{n,\alpha,\beta} s_{n\alpha}{}^{*} s_{n\beta}\chi_\alpha(x_0)\chi_\beta(x_0). \tag{A.6}$$

On the derivation of eq. (A.6), we used normalized orthogonal relation between ϕ_ns. We now assume that width of the terminal 1 is enough wide for transverse energy of fundamental mode in the terminal 1 becomes 0 and an energy filter, which is a energy barrier whose height is equal to E, is inserted between the terminal 1 and the electron wave device. Then, the expression of total current eq. (A.6) is modified to be

$$\int\left|\psi_{1\leftarrow 2}(x; x_0)\right|^2 dx = \sum_{\alpha,\beta} s_{0\alpha}{}^{*} s_{0\beta}\chi_\alpha(x_0)\chi_\beta(x_0), \tag{A.7}$$

since higher modes cannot be excited due to the energy barrier. By noticing eq. (A.2) and (A.3), we are with a conclusion of

$$\left|\psi_{2\leftarrow 1}(x_0)\right|^2 = \int\left|\psi_{1\leftarrow 2}(x; x_0)\right|^2 dx. \tag{A.8}$$

This is backing of our observation principle.

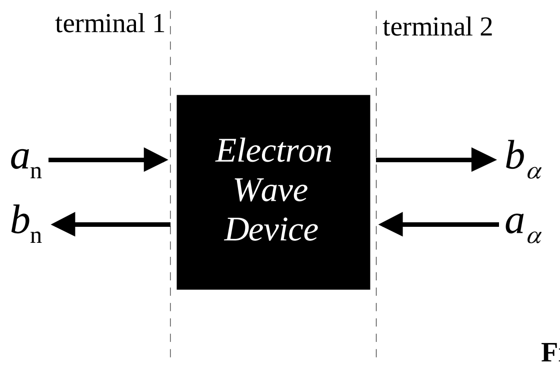

Figure A-1: Device description model